Surface Complexation Description of the Dissolution of Chromium(III) Hydrous Oxides by Oxalic Acid

Luis A. García Rodenas,[†] Alberto M. Iglesias,[†] Ariel D. Weisz,[†,‡] Pedro J. Morando,*[,†] and Miguel A. Blesa*[,†,‡]

Unidad de Actividad Química, Comisión Nacional de Energía Atómica, Avenida del Libertador 8250, 1429 Buenos Aires, Argentina, and INQUIMAE, Facultad de Ciencias Exactas y Naturales, Universidad de Buenos Aires, 1428 Buenos Aires, Argentina

Received July 31, 1997[⊗]

Aqueous oxalic acid forms surface Cr^{III}−oxalato complexes with suspended chromium(III) oxide particles; the FTIR spectra demonstrate that both carboxylate groups of the ligand are bound to surface Cr^{III}. Surface complexation is followed by changes in the surface redox potential toward more negative values and by the dissolution of the oxide. The dissolving steady state potential is in the range −60 to −210 mV against SHE. During surface conditioning, traces of oxidants at the interface are reduced, and some reduced metal ions accumulate. Minor amounts of dissolved Cr^{II} are generated and can be collected at a vicinal ring electrode set at −60 mV. In agreement, dissolution kinetics suggest that generation of Cr^{II} by ligand-to-metal charge transfer within the surface complexes produces a large increase in the rate of phase transfer, as expected from the properties of Cr^{III} and Cr^{II}. Added chromous salts also catalyze the dissolution through intervalence charge transfer within an oxalato-bridged Cr^{III}−L−Cr^{II} surface dimeric complex. The rate of dissolution at 65 °C follows a Langmuir−Hinshelwood dependence on oxalic acid concentration, a power law (order 0.31) dependence on proton concentration, and an $a + b[Cr^{II}]^{0.64}$ dependence on [Cr(II)]. The Langmuir−Hinshelwood parameters are interpreted in terms of the stability constant of the surface Cr^{III}−oxalato complex.

Introduction

The interaction of anions with metal oxides immersed in water is successfully described by the surface complexation approach, which represents chemisorption by mass-law chemical equations, corresponding to the formation of surface complexes.[1] The adsorption isotherms may be described in terms of a modified Langmuir equation that embodies the chemical affinity (surface complex stability constant) and the electrostatic contribution associated with the existence of a surface potential and an electrical double layer in the solution. A large body of stability constants for surface complexes is already available in the literature,[2] and, to a lesser extent, structural evidence on the nature of the surface complexes is also available. Much more limited is the information available on the reactivity of surface complexes; although the rates of dissolution may, in some cases, be cast in the form of first-order rate equations on the surface complexes concentration, trends in reactivity cannot be probed as usual in solution chemistry. When the driving force is adequately high, heterogeneous charge transfer is normally a fast process,[3] but these reactions cannot proceed to a large extent unless charge injection into the (insulating or insulated) solid is compensated by some type of ion transfer. Typically, either dissolution or phase transformations are required in order to render the charge transfer irreversible; these slower reactions can be described adequately in terms of the reactivity of surface complexes.

Our previous work has documented the extensive redox chemistry of iron(III) surface complexes (formed in the surface of iron oxides);[1,4−6] the labilization of pendant oxo bonds by surface complexation has also been analyzed by us, although the experimental substantiation is scarce.[1,7] The operation of charge transfer reactions in Mn(III,IV) surface complexes has also been demonstrated.[8,9] Both Fe(III) and Mn(III,IV) oxides are made sensitive to reductive dissolution because of these electron transfer reactions within surface complexes. Chromium(III) oxides undergo oxidative dissolution through a mechanism that bears close similarities with the oxidation of dissolved chromium(III);[10] these oxides are much less prone to reductive dissolution, because of the negative values of the redox potential of the Cr(III)/Cr(II) couple.

Many years ago, Taube and Myers demostrated that $CrCl_3$-(s) dissolution was catalyzed by Cr(II);[11] this catalysis is not very efficient for chromium(III) oxides, but, as we show in this paper, in combination with oxalic acid the catalytic pathway becomes important. Oxalic acid is known to interact strongly with metal oxides; this quality results from its properties as a moderately strong diprotic acid, as a strong complexant able to form stable complexes with a wide variety of metal ions, and as a thermodynamically strong reductant. Kinetic factors are limiting, as is usual for organic reductants, but activation is

[†] Comisión Nacional de Energía Atómica.
[‡] Universidad de Buenos Aires.
[⊗] Abstract published in *Advance ACS Abstracts,* December 1, 1997.

(1) Blesa, M. A.; Morando, P. J.; Regazzoni, A. E. *Chemical Dissolution of Metal Oxides*; CRC Press: Boca Raton, FL, 1994.
(2) Dzombak, D. A.; Morel, F. M. M. *Surface Complexation Modeling*; Wiley: New York, 1990.
(3) Miller, R. J. D.; McLendon, G. L.; Nozik, A. J.; Schmickler, W.; Willig, F. *Surface Electron Transfer Processes*; VCH Publishers: New York, 1995.
(4) Baumgartner, E. C.; Blesa, M. A.; Marinovich, H. A.; Maroto, A. J. G. *Inorg. Chem.* **1983**, *22*, 2224.
(5) Blesa, M. A.; Marinovich, H. A.; Baumgartner, E. C.; Maroto, A. J. G. *Inorg. Chem*. **1987**, *26*, 3713.
(6) Borghi, E. B.; Regazzoni, A. E.; Maroto, A. J. G. ; Blesa, M. A. *J. Colloid Interface Sci.* **1989**, *130*, 299.
(7) Regazzoni, A. E.; Blesa, M. A. *Langmuir* **1991**, *7*, 473.
(8) Stone, A. T.; Morgan, J. J. *Environ. Sci. Technol.* **1984**, *18*, 617.
(9) Stone, A. T. *Environ. Sci. Technol.* **1987**, *21*, 979.
(10) Reartes, G. B.; Morando, P. J.; Blesa, M. A.; Hewlett, P.; Matijević, E. *Chem. Mater*. **1991**, *3*, 1101.
(11) Taube, H.; Myers, H. *J. Am. Chem. Soc.* **1954**, *76*, 2103.

S0020-1669(97)00938-5 CCC: $14.00

Table 1. Characteristics of Both Oxides $Cr_2O_3 \cdot nH_2O$

sample	Cr content, % (w/w)	n^a	surface area, $m^2\ g^{-1}$
A	155	28	6.1
B	297	11	36.2

[a] From thermogravimetric analysis.

rather facile, either by the formation of inner sphere complexes and/or by the action of light.

This paper describes an experimental study of the interaction of oxalic acid, and of chromium(II) oxalate complexes, with chromium(III) hydrous oxides. The results demonstrate the complexation of surface chromium(III) ions by oxalate and the formation of surface mixed-valence dimeric complexes bridged by oxalate; inner electron transfer within these complexes results in oxide dissolution.

The well-known aggressiveness of oxalic acid toward iron oxides is the basis of several technological uses of this reagent, as etching and cleaning or decontaminating agent for metal surfaces on which metal oxides have grown or deposited, including stainless steels.[12] Our results demonstrate that both iron and chromium oxides are sensitive to acid solutions containing oxalate.

Experimental Section

Synthesis of $Cr_2O_3 \cdot nH_2O$. First, 30 cm^3 of 27% ammonia was added to 600 cm^3 of 0.2 mol dm^{-3} $Cr(NO_3)_3$ at 90 °C. The mixture was left at this temperature for 1 h, and afterward the precipitate was filtered off, rinsed with distilled water, and dried in an oven at 60 °C. The solid was characterized by chemical analysis, thermogravimetric analysis, and surface area (BET) measurements. Two batches were synthesized (oxide samples A and B) that differed in their water contents. Table 1 shows the characteristics of both samples.

Infrared Spectra. The infrared spectra were recorded in a Nicolet 560P spectrometer fitted with a liquid nitrogen-cooled MCT/A detector. Each spectrum was calculated from 256 scans at 8 cm^{-1} resolution. Chromium oxide layers were deposited on the horizontal surface of a 45°, 10 reflections-ZnSe ATR prism by evaporation of 50−100 μL of aqueous suspensions at room temperature; oxide spectra under water were also recorded. Blank oxalic acid solution spectra were recorded at several oxalic acid concentrations and pH values. The spectra of the oxide deposits treated with oxalic acid solutions were recorded after 40 min contact time with the appropriate solution and after rinsing the oxide several times with pure water to eliminate excess oxalic acid.

Electrochemical Experiments. (i) Open-Circuit Measurements. Pellets, 1 cm in diameter, of *ca*. 0.2 g of $Cr_2O_3 \cdot nH_2O$ (oxide B) were made in a press under a pressure of 500 kg cm^{-2}; the thickness of the pellets was around 1 mm. These pellets were connected to a wire with silver paint and immersed in epoxy resin. The working exposed face was polished with silicone carbide paper down to 600 grit before each experiment. A 0.3 dm^3 three-electrode cell, thermostated at 65.0 ± 0.1 °C, was used for the measurements, with a platinum counterelectrode and a saturated calomel reference electrode. Static potentials were measured as a function of time, using a Keithley voltmeter (Model 197 A).

(ii) Rotating Disk−Ring Array Measurements. A wire (0.02 cm diameter) coil Pt electrode surrounding an isolated oxide disk was built in an epoxy resin, as depicted in Figure 1. The oxide used was sample B. Construction details were similar to those described for the oxide electrode; in this case, however, the oxide pellet was insulated, and the whole array was connected to a drive through a shaft that maintained a constant rotation speed of 140 rpm. The electrochemical cell was again a conventional three-electrode arrangement, thermostated at 65.0 ± 0.1 °C.

Kinetic Measurements. Here, 20 mg of $Cr_2O_3 \cdot nH_2O$ was poured into a magnetically stirred solution containing adequate amounts of oxalic acid and NaOH (to yield the desired pH) in a cell provided with a jacket to circulate water at 65.0 ± 0.1 °C. The influence of ionic strength was cursorily explored to demonstrate that, in our experimental range, it did not appreciably influence the rate. The measurements were carried out in the range $0.16 \geq I \geq 0.025$ mol dm^{-3}, except for one experiment at the highest oxalic acid concentration ($I = 0.46$ mol dm^{-3}). Aliquots were withdrawn periodically and filtered through 0.45 pore size cellulose acetate membranes. Total chromium concentration was measured in the filtrate by AAS in a Varian AAR 5 apparatus. In some experiments, [Cr(VI)] was measured using the diphenylcarbazide method.[13] Experiments were performed with both oxide samples A and B. Chromium(II) chloride solutions were prepared by reduction of chromium(III) chloride with amalgamated zinc. To avoid oxidation of Cr(II), nitrogen was continuously bubbled through the solution during dissolution. The added chromium(II) concentration was determined by reaction with excess iron(III), followed by titration of the iron(II) produced with a standard potassium dichromate solution.[14]

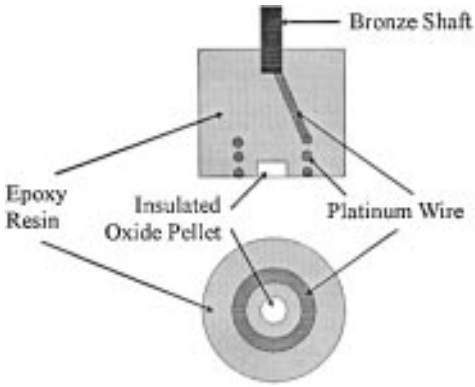

Figure 1. Schematic picture of the rotating disk−ring array.

Results

Spectral Characterization of the Interaction of Oxalic Acid and Chromium(III) Hydrous Oxide. Figure 2 shows the FTIR spectra of the two oxide samples before (a and b), and after (c and d) exposure to a solution containg oxalate (0.1 mol dm^{-3}) at pH 3.6, and of a solution containing Cr(III) (0.01 mol dm^{-3}) and oxalate (0.1 mol dm^{-3}) at pH 4.9, against a blank of 0.07 mol dm^{-3} oxalate at the same pH (e).

Oxide A (Figure 2a) presents peaks at 1560, 1470, and 1390 cm^{-1}; the first one can be attributed to surface hydroxide groups and the others to anion contamination (carbonate and/or nitrate).[15,16] In contrast, the dominant feature in the spectrum of the less hydrated sample, B (Figure 2b) is the peak centered at 1130 cm^{-1}, with shoulders at 1070 and 980 cm^{-1}, which can be assigned to tetrahedrally coordinated chromium, probably due to oxidized Cr. In agreement, Singh *et al*.[15] have reported bands due to $[CrO_4]^{n-}$ moieties in hydrous chromium oxides near 1050 cm^{-1}; Ratnasamy and Leonard[16] also attribute a band centered at 1095 cm^{-1} to dissociatively chemisorbed oxygen. The presence of oxidized chromium on the surface is not surprising; chromium oxides are readily oxidized by a variety of oxidants,[10] including oxygen.[17] The species responsible for the band at 1130 cm^{-1} is not, however, adsorbed chromate. FTIR measurements of the oxide equilibrated with CrO_4^{2-} show a peak at 905 cm^{-1}. The shift may be due to a lower oxidation state and /or different coordinative arrangement. For comparison, the $(\nu_1 + \nu_3)$ CrO_4 bands in $NaCr(CrO_4)_2$ are in the range

(12) Blesa, M. A.; Regazzoni, A. E.; Maroto, A. J. G. *Trends Inorg. Chem.* **1993**, *3*, 25.

(13) Vogel, A. I. *Química Analítica Cuantitativa*; Kapelusz: Buenos Aires, 1961; Vol. 2.

(14) Kolthoff, I. M.; Sandell, E. B. *Textbook of Quantitative Inorganic Analysis*; McMillan Co.: New York, 1952.

(15) Singh, K. K.; Sarode, P. R.; Ganguly, P. *J. Chem. Soc. Dalton Trans.* **1983**, 1895.

(16) Ratnasamy, P.; Leonard, A. J. *J. Phys. Chem.* **1972**, *76*, 1838.

(17) Farrow, C. J.; Burkin, A. R. *Leaching and Reduction in Hydrometallurgy*; The Institute of Mining and Metallurgy: London, 1970.

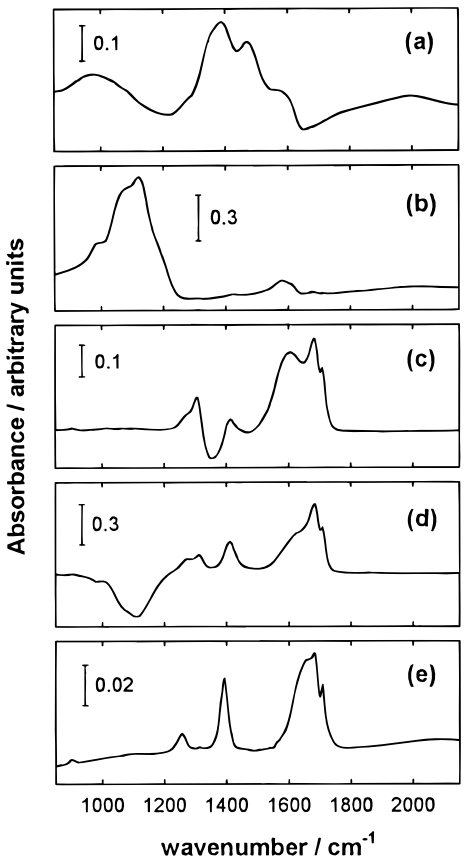

Figure 2. FTIR spectra of (a) chromium oxide A; (b) chromium oxide B; (c and d) surface complexes of oxides samples A and B, respectively, after exposure to 0.1 mol dm^{-3} oxalate solution at pH 3.6; and (e) aqueous complex of a solution containing 0.01 mol dm^{-3} Cr(III) and 0.1 mol dm^{-3} oxalate at pH 4.9 against a blank of 0.07 mol dm^{-3} oxalate at the same pH.

790−970 cm^{-1}.[18] Electrokinetic measurements demonstrate that chromate does, indeed, adsorb.[19] Sequential FTIR spectra of the oxide in oxalic acid solutions (not shown) demonstrate the gradual decrease of this band, along with the appearance of the surface oxalate bands, also in agreement with the assignment to oxidized chromium moieties.

The striking differences in the FTIR spectra of both oxides, although not surprising, demonstrate that the initial reactivity of nominally equivalent samples may differ appreciably due to the presence of impurities on the surface. Our results, discussed below, demonstrate, however, that, after surface conditioning in the initial stages of interaction with oxalic acid, both samples behave similarly.

The spectrum shown in Figure 2e corresponds to $Cr(C_2O_4)_3^{3-}$; the contribution from uncomplexed oxalate has been substracted. The peaks at 1700, 1410, and 1260 cm^{-1} coincide with the most intense vibrations in $K_3[Cr(C_2O_4)_3]$ and $K_3[Cr(C_2O_4)_2(H_2O)_2]$.[20] Free oxalate ion presents peaks at 1640 and 1320 cm^{-1} (not shown, see also ref 21).

Comparison of the spectra of the two oxide samples after interaction with oxalic acid (Figure 2c,d) with the spectrum of dissolved $Cr(C_2O_4)_3^{3-}$ (Figure 2e) demonstrates that surface complexes with chelated oxalate are formed. The main peaks (1710, 1680, 1410, and 1260 cm^{-1}) can be atributed to the ≡Cr-

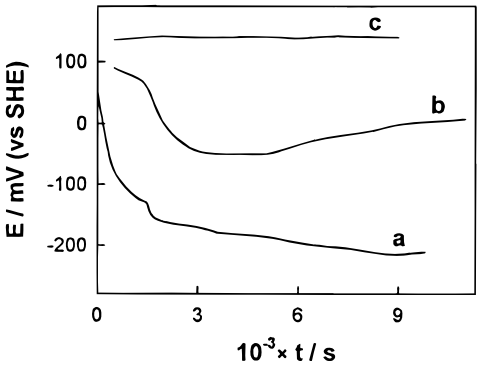

Figure 3. Time evolution of the open-circuit (corrosion) potential of the chromium oxide B pellet immersed in oxalic acid solution at pH 3.5 and 65 °C: (a) $[H_2C_2O_4] = 0.1$ and (b) 0.05 mol dm^{-3}. Also shown is the open-circuit potential time evolution in sulfuric acid at pH 3.5 (c).

(C_2O_4) moiety; in the solids $K_3[Cr(C_2O_4)_3]$ and $K[Cr(C_2O_4)_2(H_2O)_2]$, the same bands are observed.[20,21] The shoulder at 1620 and the peak at 1310 cm^{-1} indicate the presence of lesser amounts of uncoordinated oxalate, in agreement with the solution spectrum (not shown). No evidence is found of the presence of $HC_2O_4^-$ species. Although some free oxalate may remain because of incomplete washing of the solution, the peaks assigned to coordinated oxalate can be unambiguosly attributed to a surface complex. In this complex, both carboxylate groups are bound, either to the same surface Cr(III) ion or to two adjacent ones. In Figure 2d, the decrease of the peak due to chromate is significant and represents most probably the reduction of Cr(VI) by oxalate on the oxide surface. In Figure 2c, some decrease of the bands is also observed due to hydroxylated surface sites, as expected if substitution of oxalate for OH takes place.

Open-Circuit (Corrosion) Potential. Figure 3 shows that the open-circuit potential of the oxide B pellet in oxalic acid evolves toward negative values, until a plateau is achieved at values that depend on the oxalic acid concentration (for $[H_2C_2O_4] = 0.1$ mol dm^{-3} at pH 3.5, *ca.* −210 mV *vs* SHE). At lower oxalic acid concentrations, the potential does not actually reach a steady state value but drifts again to more positive values at long times. For comparison, the open-circuit potential time evolution in sulfuric acid is also shown in Figure 3.

Rotating Disk−Ring Array Measurements. The nature of the species put in solution during the dissolution in 0.1 mol dm^{-3} oxalic acid at pH 3.5 was explored using the insulated oxide disk/platinum ring array. It is assumed that the potential on the disk during this experiment is the open-circuit value of Figure 3, curve a, −210 mV. By setting the ring potential at −60 mV *vs* SHE, it was possible to measure an anodic current intensity 1 order of magnitude larger than the background value. The nature of the species involved in the anodic oxidation at the ring electrode was explored by measuring the current generated in different media: *in situ*-generated Cr(II) (by reduction of dissolved Cr(III) with zinc pellets in oxalic acid media) produced a large intensity; dissolved Cr(III) by itself, in oxalic acid media, did not produce a significant current enhancement unless a strong reductant was present; and *in situ*-produced H_2 (by zinc pellets), in the absence of Cr(III), also did not give rise to a significant current enhancement. The results, summarized in Table 2, indicate that minor quantities of dissolved Cr(II) are generated by the attack of oxalic acid on the hydrous chromium(III) oxide disk.

Dissolution Kinetics. Figure 4 shows selected examples of the extent of dissolution/time profiles obtained under different

(18) Saavedra, M. J.; Parada, C.; Baran, E. J. *J. Phys. Chem. Solids* **1996**, *57*, 1929.
(19) Magaz , G. E.; Blesa, M. A. Unpublished results.
(20) Schmelz, M. J.; Miyazawa, T.; Mizushima, S.; Lane, T. J. ; Quagliano, J. V. *Spectrochim. Acta* **1957**, *9*, 51.
(21) Hug, S.; Sulzberger, B. *Langmuir* **1994**, *10*, 3587.

Table 2. Potentiostatic Experiments Performed in a Conventional Electrochemical Cell with Cr(II) Generated *in Situ* and in the Disk−Ring Electrode at 65 °C

procedure	$I_{final}/I_{initial}$	comments
(1) platinum working electrode and counter electrode; SCE reference; potential set at −60 mV (SHE) $[H_2Ox] = 0.1$ mol dm^{-3}; $Zn^0 + HCl + Cr^{3+}$	400	*in situ* generation of Cr(II) in oxalic media produced a large current intensity
(2) platinum working electrode and counter electrode; SCE reference; potential set at −60 mV (SHE) $[H_2Ox] = 0.1$ mol dm^{-3}; $Cr^{3+} + HCl$	3	dissolved Cr(III) by itself did not produce a significant current enhancement
(3) platinum working electrode and counter electrode; SCE reference; potential set at −60 mV (SHE) $[H_2Ox] = 0.1$ mol dm^{-3}; $Zn^0 + HCl$	3	the H_2 produced by the zinc pellets did not produce a significant current
(4) addition of Zn^0 in the course of experiment 2	40	a significant current enhancement is seen upon Cr(II) generation
(5) disk-ring electrode potential set at −60 mV (SHE) $[H_2Ox] = 0.1$ mol dm^{-3}	10	no significant current is observed when the disk is isolated from the solution; otherwise, Cr(II) is generated in the dissolution process of the oxide pellet by oxalic acid and detected on the ring electrode

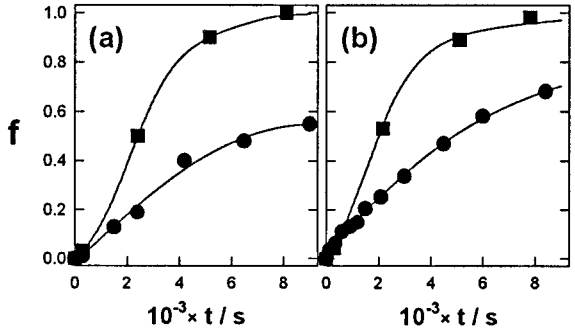

Figure 4. Dissolution profiles at pH 3.5 and 65 °C for oxide A (●) and oxide B (■): (a) 0.1 and (b) 0.28 mol dm^{-3} $H_2C_2O_4$.

experimental conditions for oxide samples A and B. Whereas many profiles are sigmoidal for oxide B, they are deceleratory for oxide A (*i.e.*, the maximum rate is the initial rate). As we shall see, important differences are expected from sample to sample in the characteristics of the initial rates; by contrast, the behavior at longer times may be described on the basis of more general ideas.

In heterogeneous kinetics, sigmoidal profiles may arise for a variety of reasons. A general empirical expression is of the form

$$df/dt = (k_a + k_b g(t))S(t) \quad (1)$$

where f is the fractional extent of dissolution, $f = (w_o - w)/w_o$ (w_o and w being the initial and instantaneous masses of undissolved solid), k_a and k_b are two empirical constants (that depend on the solution composition and on the history of the solid), $g(t)$ is a function that describes an increase with time of the rate per unit area, and $S(t)$ is the instantaneous available surface area. Fitting of experimental data to eq 1 can be done only if the functions $S(t)$ and $g(t)$ are known. In the case of the dissolution of iron oxides by oxalic acid, the sigmoidal profiles were accounted for by assuming that $S(t)$ is given by the contracting volume expression (eq 2), where S_0^s is the specific

$$S(t) = w_o S_0^s (1 - f)^{2/3} \quad (2)$$

surface area, and $g(t)$ is a function of the concentration of dissolved Fe(II). The attempt to model $g(t)$ on the assumption that it describes the buildup of dissolved Cr(II), however, could not explain the induction periods. For instance, the differences between oxides A and B seem to be determined by the original characteristics of the surface and by the possible existence of traces of oxidants. Therefore, we introduced an empirical induction time, t_0; for $t < t_0$, $(df/dt) = 0$; for $t \geq t_0$, the contracting volume rate law (eq 3) was assumed to hold; this

$$1 - (1 - f)^{1/3} = {}^1/_3 k_A w_0 S_0^s (t - t_0) \quad (3)$$

expression provides a reasonable fitting, even in cases in which there are large deviations from the assumptions of equally sized, spherical particles.[22] A good linear fitting was obtained for the dependence of $1 - (1 - f)^{1/3}$ on time, as shown in the insets of Figures 5−7; in what follows, we shall, therefore, discuss the influence of solution variables on the rate constant k_A defined by eq 3.

Equation 3 has been expressed in terms of the fractional extent of dissolution in order to derive kinetic profiles that are independent of the mass/volume ratio; k_A is a specific rate (rate per unit area, m^{-2} s^{-1}). The rate of increase in chromium concentration [Cr] is simply

$$d[Cr]/dt = (2w_o/MV)\, df/dt \quad (4)$$

where M is the molar weight of the solid $Cr_2O_3 \cdot nH_2O$, and V is the solution volume.

The linearity of the plots according to eq 3, or the constancy of k_A, implies that, after the induction period, the reaction reaches a steady state in which the rate per unit area is constant.

The reactivities of the two different samples used in this study follow similar trends, but their intrinsic reactivities are different; further, for the trivial correction for specific surface area, sample A is characterized by kinetic parameters that are *ca.* 2 times higher than those of sample B, as demonstrated, for instance, by comparison of the values for k_A at pH 3.5 and 0.1 mol dm^{-3} oxalate.

Figure 5 shows the dependency of k_A on oxalic acid concentration for oxide B at pH 3.5; the dissolution profile in sulfuric acid at pH 3.5, which shows negligible dissolution, is also included. The inset shows some of the linear profiles from which the values of k_A were derived. The dependence of k_A for oxide B on total oxalic acid concentration at pH 3.5 can be described by the Langmuir−Hinshelwood equation (eq 5), with $k_{A\,sat} = 5.5 \times 10^{-4}$ s^{-1} m^{-2} and $Q_L = 28.9$ mol^{-1} dm^3.

$$k_A = k_{A\,sat} Q_L [Ox]_T / \{1 + Q_L [Ox]_T\} \quad (5)$$

Figure 6 shows that the pH dependency of k_A in 0.1 mol dm^{-3} total oxalate concentration for oxide B is given by eq 6; again, the inset shows the plots from which k_A values were derived.

$$k_A = k_A^o [H^+]^{0.31} \quad (6)$$

At pH 0, $k_A^o = 5.0 \times 10^{-3}$ m^{-2} s^{-1}.

(22) Urrutia, G. A.; Blesa, M. A. *React. Solids* **1988**, *6*, 281.

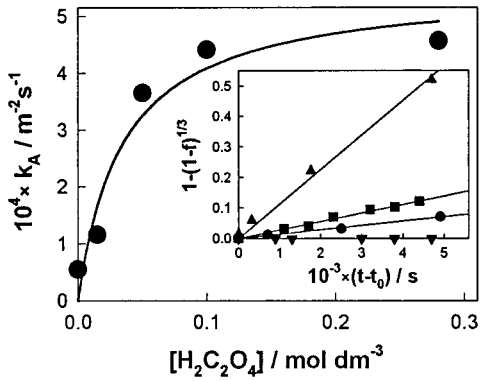

Figure 5. Dependence of k_A on total oxalic acid concentration for oxide B at pH 3.5 and 65 °C. Full line: eq 5 with $k_{A\,sat} = 5.5 \times 10^{-4}$ s^{-1} m^{-2} and $Q_L = 28.9$ mol^{-1} dm^3. Inset: some linear profiles calculated according to eq 3 for ●, 0.0052; ■, 0.015, and ▲, 0.28 mol dm^{-3} $H_2C_2O_4$; ▼, test run in H_2SO_4 at pH 3.5.

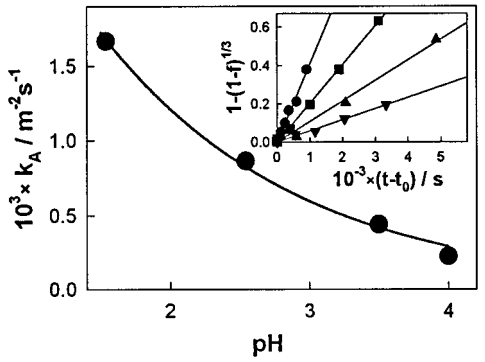

Figure 6. Dependence of k_A on pH for oxide B at $[H_2C_2O_4] = 0.1$ mol dm^{-3} and 65 °C. Full line: eq 6. Inset: linear profiles calculated according to eq 3 for pH (●) 1.54, (■) 2.54, (▲) 3.50, and (▼) 4.00.

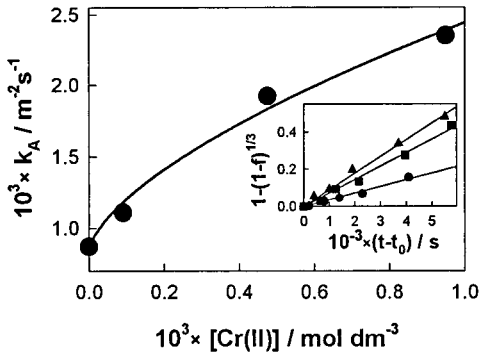

Figure 7. Dependence of k_A on Cr^{II} concentration for oxide A at pH 3.5 and 65 °C. Full line: eq 7. Inset: some linear profiles calculated according to eq 3 for [Cr^{II}] (●) 0, (■) 4.75×10^{-4}, and (▲) 9.50×10^{-4} mol dm^{-3}.

The dependence of k_A for oxide A on the concentration of added Cr(II) is shown in Figure 7. Fitting the data to a power law, eq 7, leads to $m = 0.64$, $k_0 = 8.4 \times 10^{-4}$ m^{-2} s^{-1}, $k' = 1.6 \times 10^{-3}$ (mol dm^{-3})$^{-0.64}$ m^{-2} s^{-1}. Within the data error

$$k_A = k_0 + k'[\mathrm{Cr(II)}]^m \qquad (7)$$

margins, however, a large bracket of m values yields reasonable fits.

Discussion

Surface Complexation by Oxalate. In the literature, the modes of surface complexation by oxalate have been derived indirectly from the pH dependency of the adsorption affinity[25,26] or from IR spectroscopic studies.[21,23,24] The structures proposed below for the involved surface complexes are in line with these previous reports (*cf.* ref 27).

Surface complexation requires that conditions be maintained close to electroneutrality in the coordination reaction, in order to avoid the buildup of high surface potentials. Only at low degrees of coverage may the stoichiometry of the complexation reaction deviate appreciably from the electroneutral condition. At high degrees of coverage, the stoichiometry of adsorption may be written as

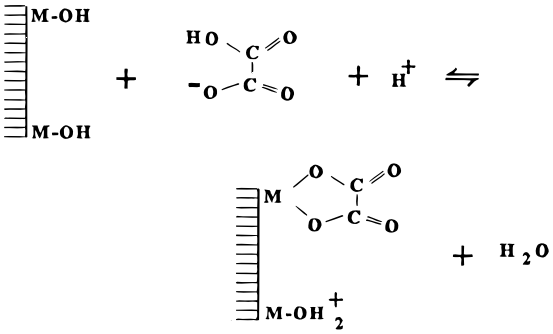

(8)

Other equivalent forms may be written; in eq 8, the surface complex was chosen to be similar to solution complexes, *i.e.*, a chelate ring formed by the deprotonated ligand and the metal ion. The symbol ≡ represents all the oxo, hydroxo, and aquo bonds required to yield a coordination number of 6; implicitly, water release or uptake from the surface is assumed, although not indicated. The dissolved oxalate species in the lhs of eq 8 is the monoanion, which prevails in the pH range 2−4. The stoichiometry of eq 8 implies coadsorption of two protons, or removal of one OH^- and adsorption of one H^+ on a vicinal M atom. The formations of the five-membered chelate ring of eq 8, or of monodentate oxalate surface complexes, are totally equivalent from the point of view of stoichiometry, as shown by the equilibrium

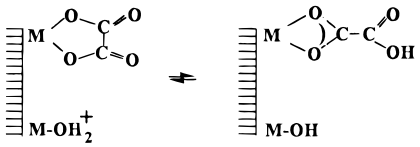

(9)

The FTIR spectra of hydrous chromium oxides equilibrated with oxalic acid solutions at pH 3.6 (see Figure 2) agree with the species depicted to the left, which is associated with a higher affinity for the surface. High oxalate concentrations, however, may drive the transformation described by eq 9, as shown in eq 10, in an adsorption mode characterized by a lower stability constant. A similar phenomenon has been observed in the adsorption of EDTA onto iron oxides.[6]

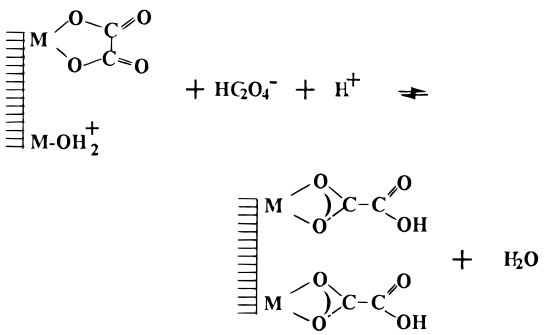

(10)

Although eqs 8 and 10 account for the stoichiometry of adsorption, oxalate chemisorption produces a negative charge

buildup on the surface, as shown by the negative values of the ζ-potentials measured by microelectrophoresis experiments.[28] This charge is due to the release of protons from M-OH_2^+ and/or from

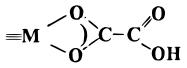

From our kinetic data, surface complexation constants can be derived, although they may correspond to species other than the main ones present on the surface; these constants are, therefore, discussed in the following paragraphs.

Phase Transfer (Dissolution) Mechanisms. (i) The Model. Any description of the dissolving interface must account for the following experimental facts: (a) the stoichiometry of dissolution, which is essentially nonreductive, Cr(III) being the main dissolved species; (b) the formation of minor quantities of Cr(II), as shown by the disk−ring array electrochemical measurements; (c) the evolution of the electrode potential until a negative plateau value is attained; (d) the shape of the dissolution time profiles, including their sigmoidal characteristics, and the influence of sample characteristics and solution variables on the steady state rate and on the induction period; (e) the quenching of the dissolution brought about by the addition of dioxygen; and (f) the formation of Cr−oxalato complexes in the surface of the oxide, as shown by FTIR spectra.

Because of the lack of accurate characterization of the real surface, some assumptions or conventions are necessary. In charged interfaces, the influence of surface potential on the rate of ion transfer is usually taken into account by assuming the existence of smooth (flat, cylindrical, spherical) interfaces; dissolution is then equated to ionic transfer between two well-defined planes, the potential difference between them being also well defined. In noncharged interfaces, a very popular model is the transfer of units from a Kossel crystal to solution, and the transformation kink → adatom, in the sequence solid bulk → surface → ledge → kink → adatom → solution bulk, is assumed to be the rate-determining step.

We shall abandon the idea of smooth interfaces, although we shall keep the equations describing the time evolution of the surface of a flat dissolving sphere in order to describe the dissolution profiles; we shall also go beyond the simple description of the Kossel units, by trying to identify surface complexes as true chemical species undergoing change. All the surface complexes are formed by a central metal ion surrounded by six ligands: oxogroups, water or hydroxide nonbridging ligands (in protolytic equilibrium), and oxalato or hydrogenooxalato, either bridging or nonbridging. The metal ions belong to the solid surface, are adsorbed in the interfacial layer, or are dissolved in the bulk liquid. Dissolution shall be assumed to be the transformation of a surface metal ion, characterized by having at least one oxo ligand, into an adsorbed ion (with no linking oxo bonds). The rate-determining step is thus associated with a bond breakage, rather than with charge transfer or ionic movement, and the electrostatic potential profile across the interface becomes unimportant in the determination of the rate. By contrast, the redox potential is of much importance; in semiconductor/water interfaces, the redox potential may be varied without affecting the electrostatic potential, because the latter is fixed by the surface protolytic equilibria, and the space charge region adjusts to changes in the Fermi level.[29] This assumption is valid as long as charge injection does not produce a change in the chemical nature of the surface. We shall discuss dissolution that is brought about by charge transfer from the solution, and we shall assume that charge injection does not produce delocalized electrons in the conduction band, but rather that surface states, corresponding to surface complexes created by adsorption, are generated in the form of aliovalent metal ions. These electron do, however, possess some mobility, and the actual site of dissolution is not necessarily that of charge injection.

Because of the properties of Cr(III) and Cr(II), we postulate that dissolution takes place by oxo bond breaking in ≡Cr(II) complexes, created by charge transfer; in agreement, O_2 addition supresses dissolution. To account for the nonreductive stoichiometry, it is required that the adsorbed Cr(II) generated by dissolution equilibrates fast with the residual surface, transferring back its electron before diffusing to bulk solution.

Charge injection from solution may be an equilibrium process (in the presence of added Cr(II) salts) or a slow, irreversible reaction (in oxalic acid solutions). Adsorption, desorption, complexation, and protolysis are also assumed to be fast.

The postulated set of reactions is, therefore,

$$\equiv\text{Cr-OH} + \text{H}_2\text{L} \rightleftarrows \equiv\text{Cr-LH} + \text{H}_2\text{O}$$

$$K_{11} = (K_8K_{10})^{1/2}K_{a1} \quad (11)$$

$$\equiv\text{Cr-LH} \rightleftarrows \equiv\text{Cr}^{\text{II}}\text{-LH}^{\bullet} \rightarrow \equiv\text{Cr}^{\text{II}}\text{-OH} + \text{LH}_2^{\bullet+} \quad (12)$$

$$\equiv\text{Cr}^{\text{II}}\text{-OH} + \text{H}_2\text{L} \rightleftarrows \equiv\text{Cr}^{\text{II}}\text{-LH} + \text{H}_2\text{O} \quad (13)$$

$$\equiv\text{Cr}^{\text{II}}\text{-LH} \rightarrow \equiv\text{Cr-LH} + \text{Cr}^{\text{II}}(\text{ads}) \quad (14)$$

$$\equiv\text{Cr-LH} + \text{Cr}^{\text{II}}(\text{ads}) \rightleftarrows \equiv\text{Cr}^{\text{II}}\text{-LH} + \text{Cr}^{\text{III}}(\text{ads}) \quad (15)$$

$$\text{Cr}^{\text{II}}(\text{ads}) \rightleftarrows \text{Cr}^{\text{II}}(\text{aq}) \quad (16)$$

$$\text{Cr}^{\text{III}}(\text{ads}) \rightleftarrows \text{Cr}^{\text{III}}(\text{aq}) \quad (17)$$

Two irreversible reactions are identified: the irreversible generation of Cr^{II} by internal electron transfer within the surface complex, followed by diffusion away from the oxidized ligand (eq 12), and the kink → adatom transition, which generates adsorbed Cr^{II} and a new exposed Cr^{III} in the surface (eq 14). The key reactive surface species, ≡Cr^{II}-LH, may be generated through eqs 12 and 15, the latter being important when Cr^{II} is added to the solution.

This scheme predicts a steady state dissolution rate (and potential) when a certain {≡Cr^{II}-LH}/{≡Cr^{III}-LH} is achieved; ≡Cr^{II}-LH accumulates during the observed induction period.

(ii) The Steady State Rate. The steady state is reached when the adsorption layer saturates in both Cr^{II} and Cr^{III}, and {≡Cr^{II}-LH} levels off through the balance of the rates of reactions 12 and 14. The steady state rate is

$$\text{d}([\text{Cr}^{\text{II}}] + [\text{Cr}^{\text{III}}])/\text{d}t = k_{14}\{\equiv\text{Cr}^{\text{II}}\text{-LH}\} = k_{12}\{\equiv\text{Cr}^{\text{III}}\text{-LH}\}$$

$$= k_{12}K_{11}\{[\text{H}_2\text{L}]/(1 + K_{11}[\text{H}_2\text{L}])\}N_s \quad (18)$$

(23) Parfitt, R.; Farmer,V.; Russell, J. *J. Soil Sci.* **1977**, *28* , 29.
(24) Parfitt, R.; Fraser, A.; Russell, J.; Farmer, V. *J. Soil Sci.* **1977**, *28*, 41.
(25) Furrer, G.; Stumm, W. *Geochim. Cosmochim. Acta* **1986**, *50*, 1847.
(26) Kallay, N.; Matijević, E. *Langmuir* **1985**, *1*, 195.
(27) Fahmi, A.; Minot, C.; Fourré, P.; Nortier, P. *Surf. Sci.* **1995**, *343*, 261.
(28) Magaz, G. E.; García Rodenas, L. A.; Morando, P. J.; Blesa, M. A. 10th Argentine Meeting on Physical Chemistry, Tucumán, Argentina, April 21−25, 1997.
(29) Morrison, S. R. *Electrochemistry at Semiconductor and Oxidized Metal Electrodes*; Plenum Press: New York, 1980.

where N_s is the total surface density of sites available for oxalate chemisorption.

Equation 18 accounts for the dependence of rate data on oxalic acid concentration (Figure 5); the pH dependence can be traced to the dependence of either k_{12} or K_{11} (or both). The dependence of the steady state rate on [Cr^{II}] is also adequately described by equilibrium 16, which predicts an increase in the value of {≡Cr^{II}-LH} when [Cr^{II}] increases. The discussion of the actual mathematical form of the adsorption isotherm is not justified, in view of the large error in the value of m (eq 7); the shape of the curve in Figure 7 is well in line with simple expectations. The role of added chromous salts is further discussed below in terms of the properties of the induction period.

The dependence of the rate on oxalic acid concentration is traced back to the complexation equilibrium 11. The Langmuir−Hinshelwood parameters in eq 5 are $k_{A\ sat} = (MV/2w_oS)$-$k_{12}N_s$ and $Q_L = K_{11}^{cond} = (K_8^{cond}K_{10}^{cond})^{1/2}K_{a1}$, where K_8^{cond} and K_{10}^{cond} are the conditional (pH-dependent) surface complexation constants for equilibria 8 and 10. The pH dependency of the constants embodies the effect of pH on both oxalic acid and surface speciation. The $Q_L$value at pH 3.5 (28.9 mol^{-1} dm^3) may be compared with some related values. Zhang *et al.*[30] reported a value of 210 mol^{-1} dm^3 for the adsorption of oxalic acid onto hematite at pH 2.7, and lower values at higher pH. For the adsorption of mercaptoacetic acid onto magnetite at pH 3.66, dissolution kinetic measurements[31] suggest $Q_L = 6.3$ mol^{-1} dm^3. Systematically, dissolution seems to be associated with surface complexation modes with low stability constants; for oxalic acid onto iron oxides, it has been postulated that the surface complex that mediates dissolution involves coordination to a single surface Fe(III) ion through one carboxylate only.[4] The evolution between different surface complexes as the concentration of the complexing anion is increased has been well documented in the case of EDTA onto magnetite.[6] This reasoning supports our interpretation of Q_L.

The dissolution rate increases monotonously with acidity, probably because the first pK_a of oxalic acid lies at pH values below the lowest spanned value (see Figure 6); this behavior is, however, to be contrasted with the bell-shaped pH dependence of the rates of dissolution of iron oxides in oxalic acid.[5] A similar case has been reported in the dissolution of magnetite by nitrilotriacetic acid.[32]

Next, we discuss the reasons for higher oxo bond breaking in ≡Cr^{II} as compared to that in ≡Cr^{III} complexes:

$$\equiv Cr^{III}\text{-}O_2CCO_2H \rightarrow \text{dissolved Cr(III)} \qquad (19)$$

Oxalate is a good electron donor that produces a trans labilizing effect. In the oxalato surface complexes, the rate of oxo bond breaking is enhanced because of the inductive effect (the increased electron density on the metal ion). A more important related effect is the increased proton adsorption produced by oxalate surface complexation. Further acid attack on the pendant oxo bonds of the vicinal iron atom is, therefore, largely enhanced. This mechanism is responsible for the dissolution of γ-Al_2O_3 and BeO in oxalic acid solutions.[25] Thus, reaction 19 could proceed through the attack by an adjacent proton on an oxo bond of a surface oxalato complex. However, the induction period and the quenching of the dissolution rate by oxygen rule out direct phase transfer. Also, it has already been shown in a previous paper[33] that direct acid attack on chromium oxides by mineral acids occurs only at much higher acidities. The first-order dependence on the surface complexes is, therefore, attributed to oxo bond breaking in surface Cr^{II} complexes.

Ligand-to-metal charge transfer (LMCT) is well known in several dissolved metal−oxalato complexes, but not in the case of Cr(III) complexes. Even though the reducing power of oxalate is adequate to generate Cr(II) from Cr(III) solutions, oxalate complexation shifts the Cr(II)/Cr(III) redox potential to more negative values, and the standard potential of the couple 20 is calculated to be $E° = -0.92$ V *vs* SHE. Hydrogen evolution under these conditions precludes the direct observation of the electrochemical reduction of tris(oxalato)chromate-(III).[34]

$$Cr(C_2O_4)_3^{3-} + e \rightleftarrows Cr(C_2O_4)_2^{2-} + C_2O_4^{2-} \qquad (20)$$

Thus, the appearance of Cr(II) cannot be attributed to reactions in solution[35] (*cf.* with the redox labilization that operates in the dissolution of iron oxides, where dissolved Fe-(II) may arise by charge transfer in surface complexes, prior to dissolution, or by photolysis of dissolved Fe(III)−oxalato complexes).[36] The measured steady state open-circuit potential corresponds to very low Cr(II) concentrations; the reduced metal ion is essentially not transferred to solution before it is reoxidized by another surface Cr^{III} complex, and a nonreductive dissolution stoichiometry results:

$$Cr_2O_3{\cdot}nH_2O + 6HC_2O_4^- \rightleftarrows 2Cr(C_2O_4)_3^{3-} + (3+n)H_2O \qquad (21)$$

By contrast, in the case of iron oxides, Fe(II) may be put in large amount in solution, as found at high temperatures.[37]

Equation 12 has been written as an irreversible reaction. In fact, following LMCT within the surface complex, either reverse charge transfer or scavenging of the oxidized $HC_2O_4^{\bullet}$ radical may take place. In the case of iron(III) dissolution by thiocyanate and iodide, the rate of dissolution is, in fact, controlled by the scavenging of the oxidized ligand.[38]

After irreversible generation of surface Cr^{II}, phase transfer rates determine the reduced surface metal ion concentration, which may range from very low values to those corresponding to a totally reduced monolayer (see ref 3 for a detailed discussion); dissolution of hydrous chromium oxides corresponds to the first case. The open-circuit potential decrease during the initial stages agrees with the reductive process. Shoesmith *et al.*[39] have shown that the corrosion potential for the dissolution of magnetite in oxalate−EDTA media is sensitive to the concentration of Fe(II) at short times, to become independent of this variable once the steady state corrosion potential is established. They concluded that a small concentration of Fe(II) is required in order to stabilize the reducing conditions (magnetite contains structural Fe(II) that is released during the autoacceleratory stage).[4,5]

(30) Zhang, Y.; Kallay, N.; Matijević, E. *Langmuir* **1985**, *1*, 201.
(31) Borghi, E. B.; Morando, P. J.; Blesa, M. A. *Langmuir* **1991**, *7*, 1652.
(32) Hidalgo, M. del V.; Katz, N. E.; Maroto, A. J. G.; Blesa, M. A. *J. Chem. Soc., Faraday Trans. 1* **1988**, *84*, 9.
(33) Reartes, G. B.; Morando, P. J.; Blesa, M. A.; Hewlett, P. B.; Matijević, E. *Langmuir* **1995**, *11*, 2277.
(34) *Encyclopedia of Electrochemistry of the Elements, Vol. IX, Part B, Chromium*; Bard, A. J., Ed.; Dekker: New York, 1986.
(35) Spinner, T.; Harris, G. M. *Inorg. Chem.* **1972**, *11*, 1067.
(36) Litter, M.; Baumgartner, E. C.; Urrutia, G. A.; Blesa, M. A. *Environ. Sci. Technol.* **1991**, *25*, 1907.
(37) Sellers, R. M.; Williams, W. J. *Discuss. Faraday Soc.* **1984**, *77*, 265.
(38) Ali, S. P.; Blesa, M. A.; Morando, P. J.; Regazzoni, A. E. *Langmuir* **1996**, *12*, 4934.
(39) Shoesmith, D. W.; Mancey, D. S.; Doern, D. C.; Bailey, M. G. *Corrosion NACE* **1989**, *45*, 149.

In the presence of added Cr(II), the buildup of $\equiv Cr^{III}$-LH is due to Cr(II)−Cr(III) charge transfer in dimeric surface complexes between surface Cr^{III} and adsorbed Cr^{II}, bridged by oxalate, rather than to LMCT. Formation of ligand-bridged binuclear surface complexes of this type is well known and has been described as *ligand-like* metal complex adsorption;[3] the participation of binuclear mixed-valence surface complexes in metal oxide dissolution is very general. Chemisorption of Fe(II) mediates iron oxides dissolution in oxalic acid,[4] and long ago Zabin and Taube[40] demonstrated the operation of electron transfer in the reductive dissolution of a series of oxides containing easily reducible metal ions, such as Co_2O_3, PbO_2, and MnO_2. In chloride media, Cr(II) dissolves reductively iron oxides; $Cr(bipy)_3^{2+}$ also dissolves these oxides.[41] The mechanism involves the adsorption of Cr(II) in the ligand-like form, *i.e.*, through a chloride bridge,

$$\equiv Fe^{III}\text{-}OH + ClCr^{+} + H^{+} \rightleftarrows \equiv Fe^{III}\text{-}Cl\text{-}Cr^{II\,2+} + H_2O \quad (22)$$

or through the formation of an outer sphere ion pair,

$$\equiv Fe^{III}\text{-}OH + Cr(bipy)_3^{2+} \rightleftarrows \equiv Fe^{III}\text{-}OH\cdots(bipy)_3Cr^{2+} \quad (23)$$

where the term "ion pair" is used loosely, to denote the close association, mediated by nonspecific forces such as hydrogen bonds, hydrophobic interactions, and eventually electrostatic forces.[42] The charge on the surface has not been specified in eqs 22 and 23; it is pH dependent and may be modified by ionic adsorption.

Thus, Cr(II) generated by the reaction, or added as a chromous salt, may chemisorb onto chromium oxide through an oxalato bridge:

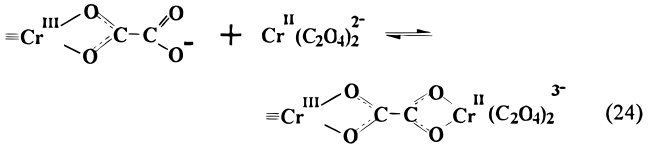

(24)

This bridged surface complex is similar to those that mediate electron transfer reactions involving Cr(II) and oxidized metal ions such as Co(III) in solution; analogously, it mediates dissolution:

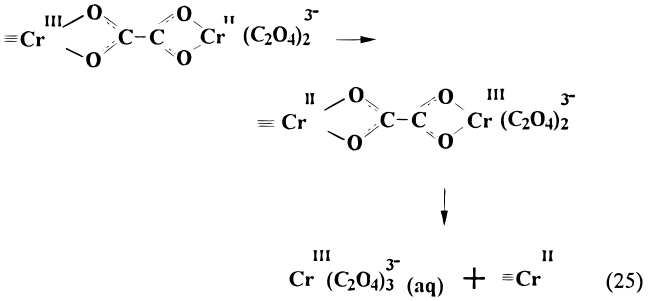

(25)

The overall process of eqs 24 and 25, followed by eq 14, leads to the stoichiometrically nonreductive, electron transfer-catalyzed dissolution. The steady state rate is now given by eq 26, which accounts for the empirical rate of eq 7:

$$d([Cr^{II}]+[Cr^{III}])/dt = k_{14}\{\equiv Cr^{II}\text{-}LH\} = [k_{12} + k_{25}K_{24}[Cr(C_2O_4)_2^{2-}]/(1 + K_{24}[Cr(C_2O_4)_2^{2-}])]\{\equiv Cr^{III}\text{-}LH\} \quad (26)$$

The rate enhancement is defined by an enrichment in interfacial Cr^{II}, *i.e.*, through the establishment of more strongly reducing conditions.

(iii) The Induction Period. The steady state potential and the steady state rate in experiments carried out with oxide B are not established in totally equivalent time spans; the difference, however, can be safely attributed to the different experimental conditions. Several different phenomena are involved in the surface conditioning. First, surface complexation may not be "instantaneous", although in many cases fast kinetics have been assumed.[43] Second, the proposed mechanism itself leads to a sigmoidal behavior, associated with the two consecutive steps 12 and 14. The observed strong dependence of the induction period on the nature of the oxide (sample A *vs* sample B) require, however, that the induction period be related with the establishment of a negative surface redox potential; because of the high reducing power of Cr(II), it is probable that pathways of destruction of this species operate, associated either with dissolved impurities and/or with oxidizing species in the surface or in the solid bulk. Oxide B presents FTIR bands typical of oxidized chromium, and the induction period is clearly observed; the quenching of dissolution by dioxygen may be viewed as a limiting case of a very long induction period. We have measured the rate of dissapearance of oxalic acid in oxygenated suspensions of hydrous chromium oxide, in an attempt to demonstrate the occurrence of a heterogeneous catalytic oxidation; although the results were negative, low rates, undetectable by us, suffice to account for the induction period.

Conclusions

We have shown earlier[10] that the well-known oxidative dissolution of chromium(III) oxides results from surface reactions between $\equiv Cr^{III}$ and oxoanions, the overall mechanism bearing similarities with the mechanism of oxidation in solution. Now we show that surface oxalate complexation also resembles the corresponding solution chemistry; the most striking difference is the occurrence, to a minor extent, of a LMCT process in the surface oxalato−chromium(III) complexes that dominates the kinetics of the dissolution reaction. The postulation of Cr(II) generation in the surface by oxalate reduction provides a coherent description of the results. The alternative mechanism, involving the redox generation of Cr(II) in the dissolved state, is unlikely. Dissolved chromium(III)−oxalate complexes are known to be stable toward redox decomposition, and furthermore, the ring electrode does not collect any current when the oxide disk is masked out, even if dissolved Cr(III) and oxalate are present (Table 2).

Acknowledgment. The authors thank Prof. M. Tudino for AAS facilities and Prof. E. Calvo for the use of the FTIR spectrometer. P.J.M. and M.A.B. are members, and A.D.W. is fellow, of the National Research Council of Argentina (CONICET). This work was supported by Comisión Nacional de Energía Atómica and by grants from University of Buenos Aires, Fundación Antorchas, and CONICET.

IC9709382

(40) Zabin, A. B.; Taube, H. *Inorg. Chem.* **1964**, *3*, 963.
(41) Segal, G.; Sellers, R. M. *Advances in Inorganic and Bioinorganic Mechanisms*; Sykes, A. G., Ed.; Academic Press: London, 1984; Vol. 3, p 97.
(42) Elliot, H. A.; Huang, C. P. *J. Colloid Interface Sci.* **1979**, *70*, 29.
(43) Stone A. T.; Morgan, J. J. *Aquatic Surface Chemistry*; Stumm, W., Ed.; Wiley-Interscience: New York, 1987; Chapter 9.